ELSEVIER

Journal of Nuclear Materials 257 (1998) 1–14

journal of nuclear materials

The observation of enrichment of O and Zr and depletion of Nb in the near surface region of a β-(Zr–20%Nb) alloy

Chunsi Zhang, Peter R. Norton *

Departments of Chemistry and Physics, Interface Science Western, The University of Western Ontario, London, Ontario, Canada N6A 5B7

Received 26 January 1998; accepted 12 May 1998

Abstract

Thermal treatment of β-(Zr–20%Nb) alloy results in the redistribution of Zr, Nb and dissolved oxygen impurity at the surface and eventually over depths of 100's of nm. Initially at $200 < T < 300$°C, only the segregation of oxygen occurs to the top 2 or 3 atomic layers (<few nm). At higher temperatures the surface concentration of Zr also increases, while the Nb concentration decreases. Depth profiling shows that beneath the segregated region, there exists a Nb-depleted and Zr-enriched region that extends over ~ 100 nm. The depth over which this region extends increases with annealing time and temperature. The driving force for the observed changes of concentration in the surface region during annealing is discussed. The diffusion coefficient of oxygen in the β-(Zr–20%Nb) alloy at 175–300°C is obtained from the kinetics of segregation which yielded a value of 6.9×10^{-5} exp(−35720 cal/RT) m^2/s.

1. Introduction

Zr–2.5%Nb alloy is widely used as the material from which pressure tubes (PTs) in CANDU (Canada Deuterium Uranium) nuclear reactors are made. The tubes are manufactured by extrusion at about 800°C followed by a final 25% cold-draw, resulting in a plate-like grain structure and texture. The microstructure of the PT is composed of grains of the α-phase (hexagonal closed-packed, 1%Nb) surrounded by a network of filament-like β-phase (body-centred cubic, 20%Nb). A final autoclaving treatment, which consists of heating in steam at 400°C for one day, is then applied to produce a protective oxide film, a few micrometers thick on the PT surface [1]. The PT which is designed to serve in-reactor for more than 20 years, is operated at 245–295°C. It has been found [2,3] that the microstructure of the tubes changes after the treatments and/or after a long time in service. Recently, increasing attention has been paid to an important microstructural change – the segregation of impurities to the grain boundaries. It has been reported that Fe, one of the common impurities, segregates to the grain boundaries after these treatments and/or long periods of reactor operation [4]. We have studied Fe segregation to the surface of single crystal α-Zr; the results of that study are consistent with the observation of Fe segregation at grain boundaries in the Zr–2.5%Nb alloy PTs [5,6]. However, Fe is not the only impurity to accumulate at the free surface of a sample, or to the grain boundaries upon heating. We have found that hydrogen and deuterium also exhibit a very strong tendency to segregate to the surfaces of Zr–2.5%Nb alloys [7,8]. In this paper, we will report on observations (by surface analytical techniques) of *enrichment* of Zr and O and an accompanying *depletion* of Nb in the near surface region of the β-Zr(20%Nb) alloy during annealing at various temperatures.

Although the β-phase (Zr–20%Nb) only constitutes about 10% by volume in Zr–2.5%Nb alloy, its network of filament-like structures and its unique properties have a significant influence on alloy performance. The observation of coupled enrichment and depletion phenomena reported in this paper is limited to studies of the *free* surface of β-Zr(20%Nb) alloy, because technical

* Corresponding author. Fax: +1-519 661 3022; e-mail: pnorton@uwo.ca.

0022-3115/98/$ – see front matter
PII: S0022-3115(98)00432-2

difficulties make a study of these properties at grain boundaries in the β-phase in a PT beyond our present capabilities. The expected similarity of structures at a free surface and at a grain boundary interface, provides relevance to the present study, although the thermodynamic and kinetic behaviours might be slightly different.

2. Experimental

The experiments were carried out in a two-level ultrahigh-vacuum equipped with a number of surface analytical techniques, including Auger electron spectroscopy (AES) and static and dynamic secondary ion mass spectroscopy (SSIMS and DSIMS). The general experimental arrangement has been described earlier [9]. The base pressure in the chamber (5×10^{-11} Torr) was achieved by using trapped diffusion and Ti-sublimation pumps.

The samples of the β-Zr(20%Nb) alloy were provided by the Chalk River Laboratory of AECL. The composition of these alloy samples, including the impurities, is listed in Table 1. The concentrations of impurities are in the range for a commercial Zr–2.5%Nb alloy. The samples were cut into approximately $5 \times 5 \times 1$ mm^3 pieces and then polished by sand paper of 400 A grade. They were then spot welded to two platinum wires which acted as sample supports, heaters and thermal conductors for cooling. The ends of these platinum wires were spot welded to two Ni-plated copper posts welded to a UHV manipulator filled with liquid nitrogen. The sample could thereby be resistively heated by passage of a current through the Pt wires, and also cooled via the copper posts and the same platinum wires. A programmable temperature controller allowed for linear temperature ramps as well as isothermal experiments. The temperature was measured by a Ni–Cr/Ni–Al thermocouple spot welded to the edge of the samples. The sample temperature could be controlled with an accuracy of better than ±0.5°C. The as-received samples, after being mounted in the chamber, were sputtered by a 3 keV, 10 nA/mm^2 Ar^+ ion beam to remove the oxide and other contaminants on the surface. Before each experiment the β-Zr(20%Nb) alloy sample was heated to 820°C and held at that temperature for a few minutes; this not only resulted in the dissolution of any remaining surface contaminants but also in the formation of a single β-phase. After the 820°C heating, the β-Zr(20% Nb) alloy sample was quenched to low temperatures at a rate of about 100°C/s; this maintained the β-phase microstructure without transformation [1]. After the annealing and quench procedure, some Zr, O etc. which are the segregants of interest in the present study, accumulated at the surface and Nb was depleted in the near surface region over a depth of a few atomic layers (one atomic layer is about 0.25 nm). The sample was briefly sputtered with Ar^+ ions before each experiment to remove the segregated layers and to produce a surface composition characteristic of the bulk.

The surface composition was measured by AES using a computer controlled single pass cylindrical mirror analyser (CMA) with a modulation voltage of 1 V. A 3 keV primary electron beam with about 1 μA current was employed for the AES experiments. The stability of the beam current was controlled to $<\pm 3\%$ in each experiment. Therefore, the stability of AES signals was also controlled to $<\pm 3\%$, important in the quantification of the amount of the relevant elements in the sampling region during the entire experiment (see below). The electric field resulting from the passage of the heating current through the platinum support wires affects the intensities of different Auger electrons by different amounts. Separate experiments were carried out to measure the effect of the heating current on the intensities of the Auger transitions used in these measurements, and all experimental data then were corrected for these effects. Surface composition was obtained by using the methods published in the AES handbook [10]. The depth profiles were measured by AES measurements acquired during ion sputtering. The sputtering rate on the sample was obtained from the sputtering rate for a ZrO_2 oxide film formed at 90 K on the sample before each profiling experiment. It has been found in previous work that the thickness of this oxide film formed at 90 K is 1.5 nm; this thickness is quite reproducible from run to run [11]. The ratio of the sputtering rate between metal and the oxide of Zr and its alloy has been measured to be 2.1 [12].

The change of O^- ion yields during the segregation experiments was measured by static secondary ion mass spectrometry (SSIMS), using a 3 keV Cs^+ ion beam with a very low current density ($\sim$0.1 nA/mm^2); this ensured that only a few percent of surface was disturbed by the Cs^+ beam during an entire experimental measurement [13]. The conversion of the O^- ion yields to the surface concentration of oxygen was done by comparing the AES O (KLL) signals obtained in parallel segregation and exposure experiments carried out under identical

Table 1
Composition of β-Zr(20%Nb) alloy (in w/w)

Elements	Nb	C	Cu	Fe	Hf	O
Concentration (w/w)	19.9%	186 ppm	90 ppm	630 ppm	95 ppm	0.135–0.194%

conditions. Because of its rapid sampling time, which gives better data statistics, SSIMS rather than AES was used to monitor the change of surface oxygen concentration (via the O^- ion yields) during segregation experiments. The measurements to be reported were reproducible on a number of samples treated as described above.

3. Results and discussion

Fig. 1 shows two Auger electron spectra. Spectrum (a) was taken from the clean sample surface, where all the segregants and contaminations have been removed from the surface by Ar^+ ion sputtering. This surface concentration is essentially the same as the bulk concentration because the sputtering rates of Zr and Nb are very similar [14]. Spectrum (b) was taken after heating the clean sample to 820°C and then quenching to room temperature. An obvious difference between these two spectra can be seen in Fig. 1: the intensities of Auger transitions from Zr and O have increased and those related to Nb have almost disappeared, indicating a depletion of Nb and an enrichment of Zr and O at the surface of the β-Zr(20%Nb) alloy upon heating and quenching.

3.1. Surface composition changes during linear heating and cooling

Fig. 2 shows the changes in the surface composition of an originally clean surface, observed during heating from room temperature to 820°C at a linear rate of 1°C/s. There is no detectable change in surface composition below 200°C. With increasing temperature from 200 to 300°C, the surface concentration of oxygen increased from 2% to 8%. The partial pressures of oxygen or oxygen containing impurities (e.g. CO, CO_2, H_2O) in the chamber were too low ($<1 \times 10^{-11}$ Torr) to account for the increase in surface oxygen concentration. Therefore, the oxygen atoms that accumulated on the surface must come from the bulk alloy by processes of diffusion and segregation. In the same temperature region, the surface concentrations of Zr and Nb decreased, whereas the intensities of their Auger transitions *remained almost constant* (Fig. 3). The segregated oxygen atoms presumably occupy interstitial sites without forming an oxide and the oxygen concentration is not so high as to significantly attenuate the Auger signals of Zr and Nb. The almost constant intensities of the Auger signals from Zr and Nb, must therefore indicate very little diffusion to or from the surface of either element. The reduction of the *concentrations* of both Zr and Nb derived from the AES data,

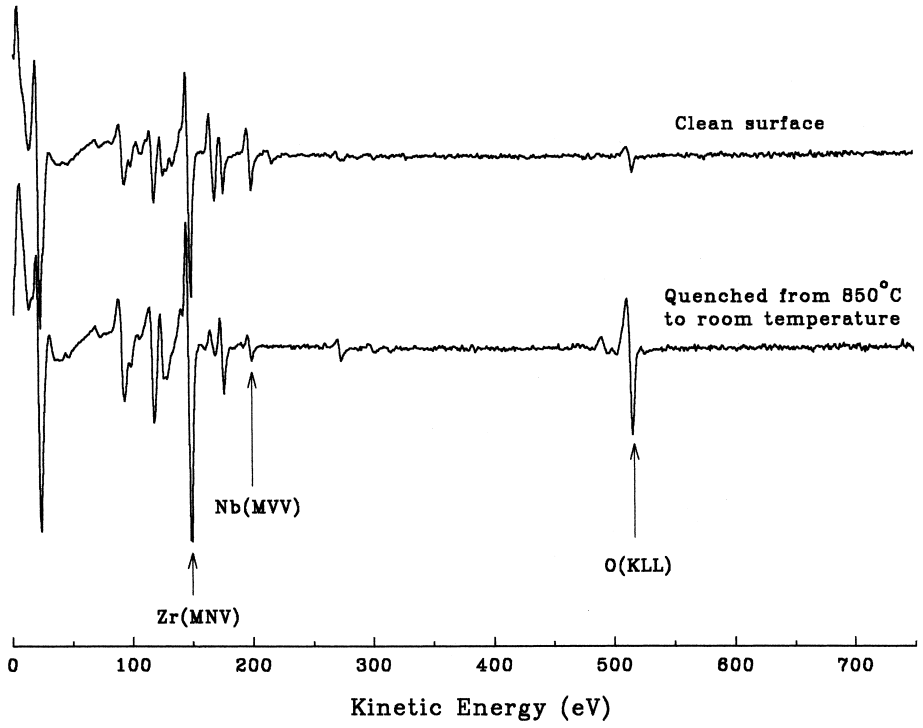

Fig. 1. Auger electron spectra from surfaces of β-(Zr–20%Nb) alloy: (a) clean, and (b) after heating to 820°C and then quenched to room temperature.

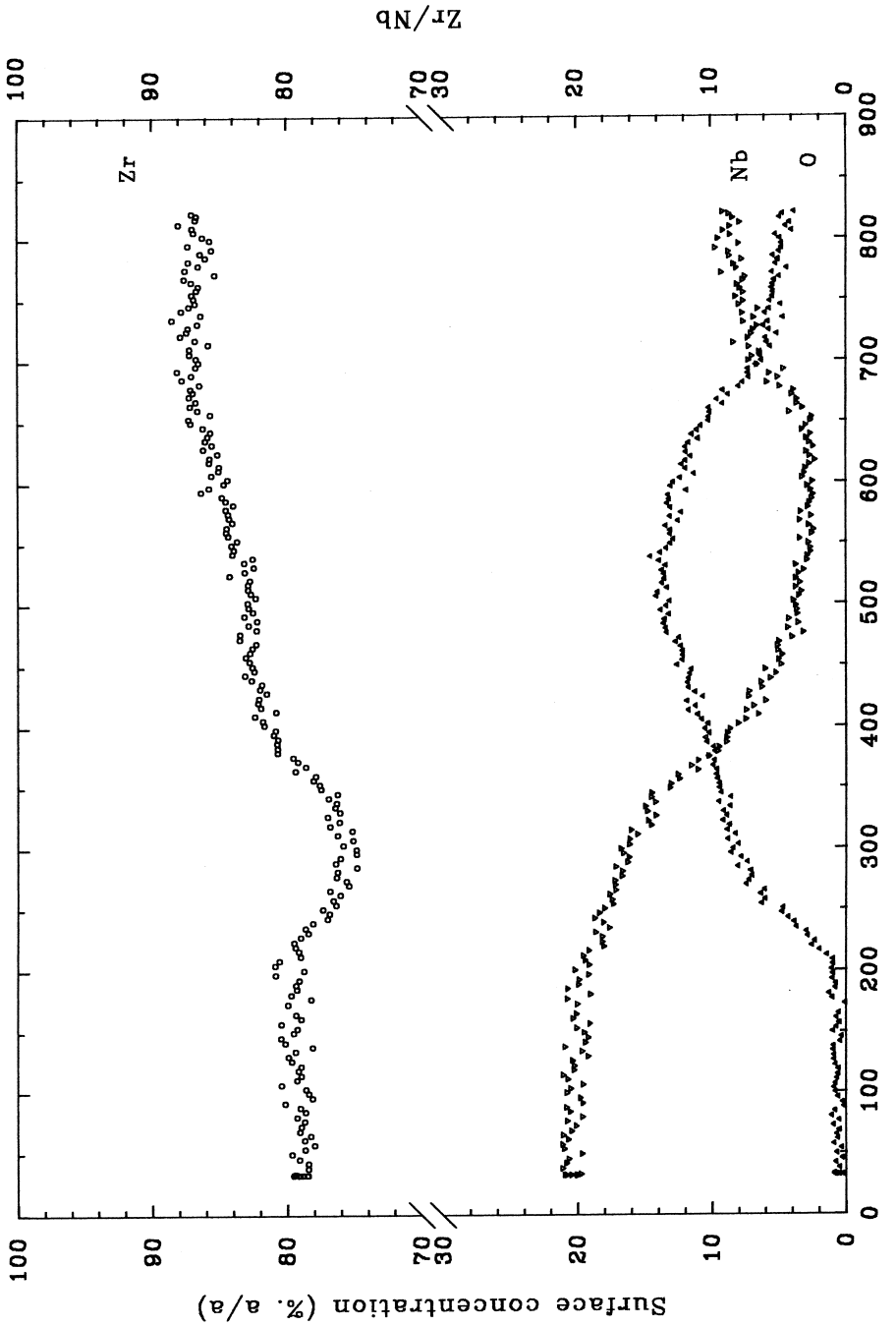

Fig. 2. Changes of concentration of Zr, Nb and O on the surface of β-(Zr–20%Nb) alloy during heating at a linear rate of 1°C/s.

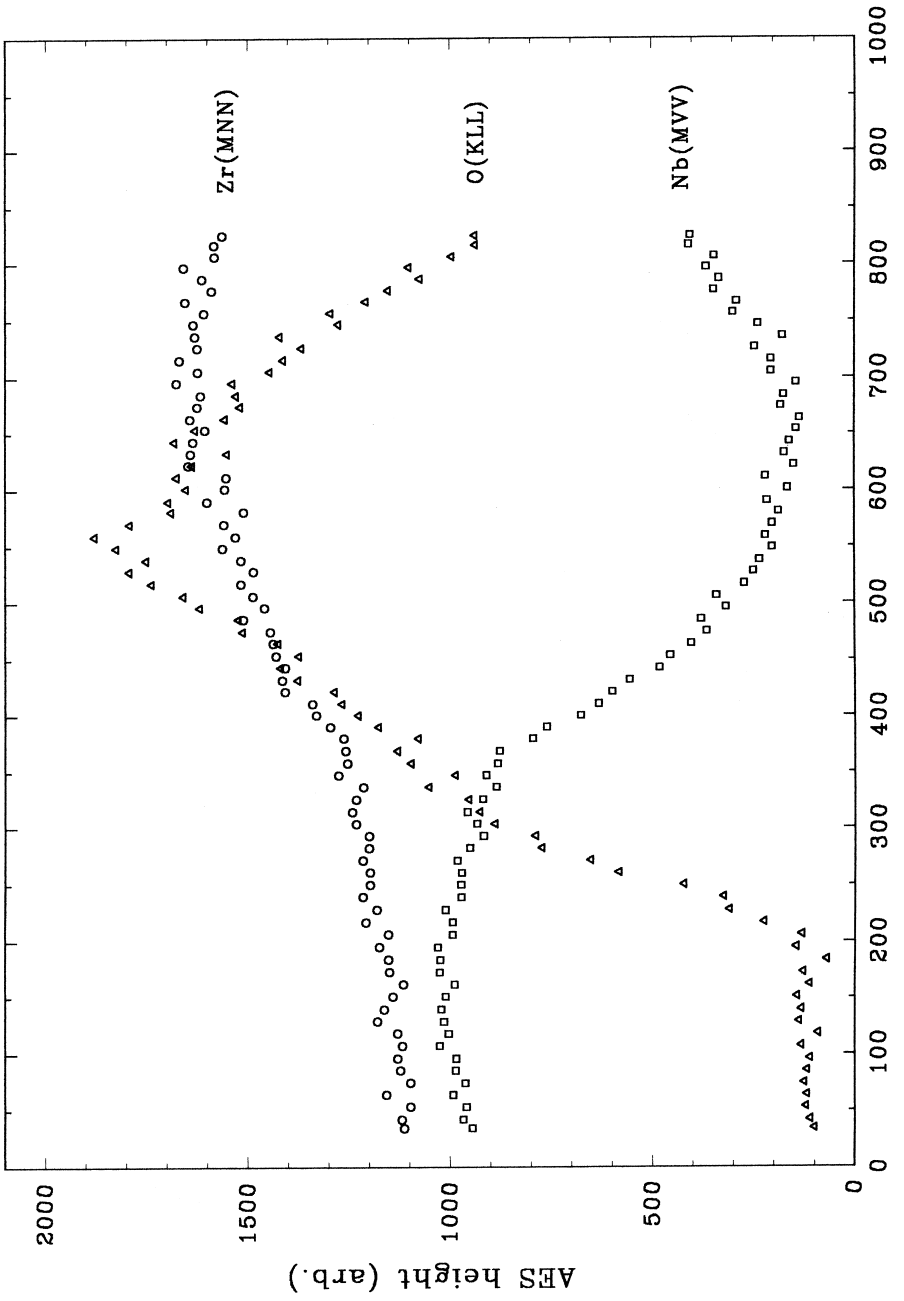

Fig. 3. Changes of intensities of Auger transitions of Zr(MNV), Nb(MVV) and O (KLL) on the surface of β-(Zr–20%Nb) alloy during heating at a linear rate of 1°C/s.

shown in Fig. 2, is due to the increase of the atomic fraction of O in the surface region. Depth profiles obtained after heating to these temperatures indicated that oxygen essentially accumulated in the first few atomic layers of the surface region with no accompanying changes in the intensities of Auger transitions from Zr and Nb. The most significant phenomenon occurring between 200 and 300°C is therefore the segregation of oxygen to the surface.

With increasing sample temperatures over 300°C, the oxygen surface concentration continually increased and reached a maximum of 13% at 550°C, then decreased to 5% at 820°C. The Zr concentration reached its maximum value of 87.5% and Nb its minimum value of 2.5%, respectively, at about 650°C. With further increase of temperature, the Zr surface concentration remained almost constant, while the Nb concentration recovered slightly reaching a value of about 7% at 820°C (Fig. 2). Since no evaporation or deposition of any element was detected (by line-of-sight mass spectrometry), all changes of surface concentration in this temperature region must also have been caused by the migration of atoms from the surface to the bulk or vice-versa.

The behaviour of oxygen in the higher temperature region (>300°C) also mainly exhibits the characteristics of segregation, because our depth profiling data (see below) showed that the oxygen concentration decreased sharply over the first few atomic layers near the surface. The further increase in the surface O-concentration with increasing temperature (300–550°C) can be partly explained by an increased diffusion rate of oxygen from the bulk to the surface, but when one considers that on α-Zr oxygen tends to *dissolve* in this temperature range, we have to consider additional thermodynamic driving forces, such as real differences in the behaviour of oxygen in the α and β phases. The reduction of oxygen concentration at still higher temperatures (>550°C) can be partially rationalized in terms of the reduction of segregation energy on the surface and increasing tendency to dissolution, which is typical behaviour for surface segregation [5–8].

With increasing temperature over 300°C, the intensities of the Zr and Nb Auger transitions are no longer constant, indicating the occurrence of migration of these two elements (Fig. 3). The concentration of Zr first increased slightly, resulting from migration from the bulk to the surface, reaching a maximum of surface concentration at 650°C. Redissolution occurred to a small extent when the temperature was further increased. By contrast, Nb atoms in the surface region start to exhibit significant migration from surface into the bulk with increasing temperatures above 300°C. Less than 25% of the original Nb surface atoms remain on the surface at a temperature of 650°C. With further increase of temperature from 650°C to 820°C some of Nb returned to the surface.

Fig. 4 shows the changes of surface concentration during cooling from 820°C to room temperature at a linear rate of 1°C/s. With decreasing temperature, oxygen resegregated to the surface, and reached a concentration of ~ 10% during cooling to room temperature; this is slightly lower than the maximum concentration observed during the heating cycle (13%). This is somewhat different from typical surface segregation behaviour [5–8]. The intensity of the Zr(MNV) transition increased slightly and the Nb(MVV) transition decreased slightly in the higher temperature region (above 700°C) and then remained constant upon cooling to room temperature. This indicated a tendency for the migration of Zr atoms towards, and Nb atoms away from the surface, respectively, in the higher temperature region. Therefore, the surface composition at room temperature is essentially very close to that formed at high temperature. Figs. 2 and 4 show that the surface concentration changes significantly after heating and cooling compared to the clean surface: Zr: from 80% to 86% Nb: from 20% to 4% and O: from 0% to 10%.

3.2. Oxygen diffusion coefficients

The surface composition during annealing at various constant temperatures (175–300°C) and for various times has been measured. Use of low annealing temperatures, (<300°C), resulted mostly in the segregation of oxygen, the Zr and Nb atoms remaining in place. In this case, the only changing concentration gradient involves oxygen, and hence the diffusion coefficient of oxygen can be deduced from the kinetics of surface segregation in this temperature region. A method has been developed to obtain the diffusion coefficient of a segregant from the change of its surface concentration during a linear heating ramp, or at various constant temperatures in isothermal experiments. This method has been successfully applied in a number of segregation systems and has been described in earlier studies [5–8]. Eq. (1) is the relevant formula to obtain the diffusion coefficients by using this method:

$$\Theta_s = [1 + 2(Dt/\pi a^2)^{0.5}]\Theta_b, \tag{1}$$

where Θ_s and Θ_b are the oxygen concentrations at the surface and in the bulk, respectively. Θ_s was determined by calibrated SSIMS measurements (Fig. 5). Θ_b is shown in Table 1. The symbol, t, is the elapsed time at a particular temperature for a given surface O concentration, and D is the diffusion coefficient. The diffusion coefficient can be readily obtained from the slope of Θ_s versus $t^{0.5}$. Fig. 5 shows the segregation rates of oxygen at 175°C, 200°C, 225°C, 250°C, 275°C and 300°C measured by SSIMS. The diffusion coefficients of oxygen deduced from the experimental results in Fig. 5, are listed in Table 2. Fig. 6, which shows the oxygen diffu-

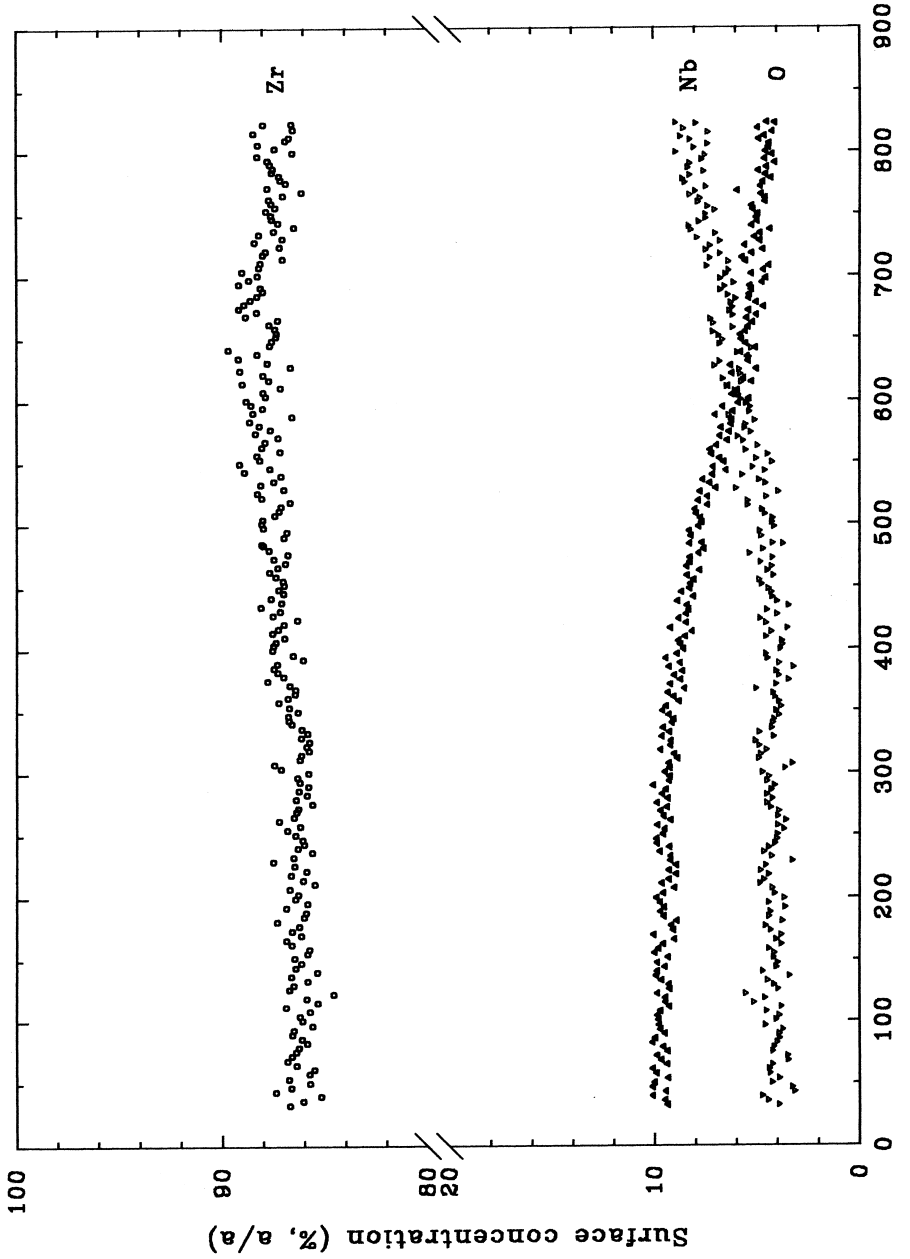

Fig. 4. The changes of concentration of Zr, Nb and O on the surface of β-(Zr–20%Nb) alloy during cooling at a linear rate of 1°C/s.

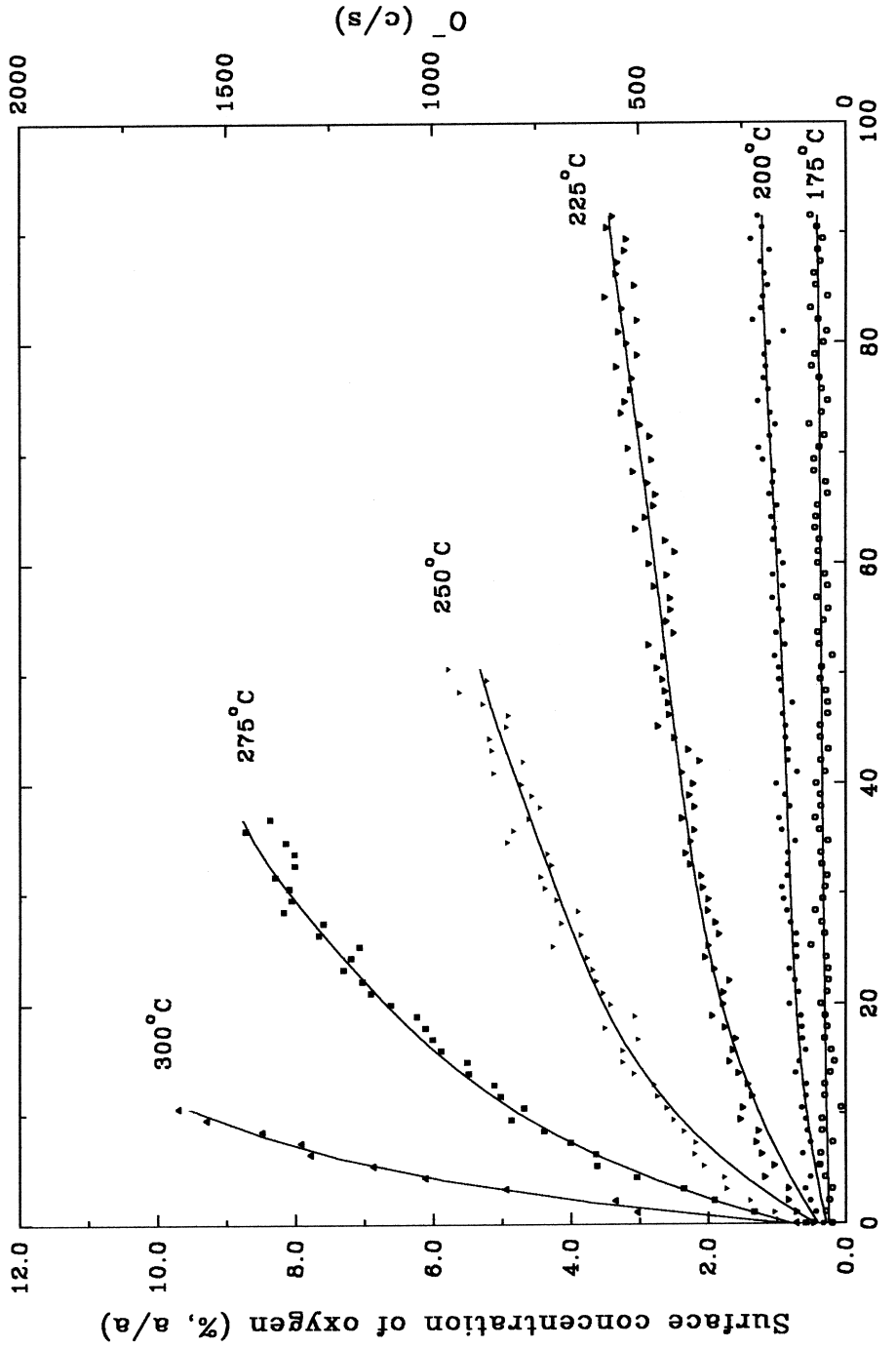

Fig. 5. The changes of surface concentration of oxygen during isothermal annealing experiments at 175°C, 200°C, 225°C, 250°C, 275°C and 300°C.

Table 2
Oxygen diffusion coefficients (D) deduced from the rate of segregation

Temperature (°C)	175	200	225	250	275	300
D (m^2/s)	3.31×10^{-22}	1.34×10^{-21}	1.69×10^{-20}	9.20×10^{-20}	3.74×10^{-19}	1.14×10^{-18}

$D = 0.69 \times 10^{-5} \exp(-35\,720\ \text{cal}/RT)\text{m}^2/\text{s}$.

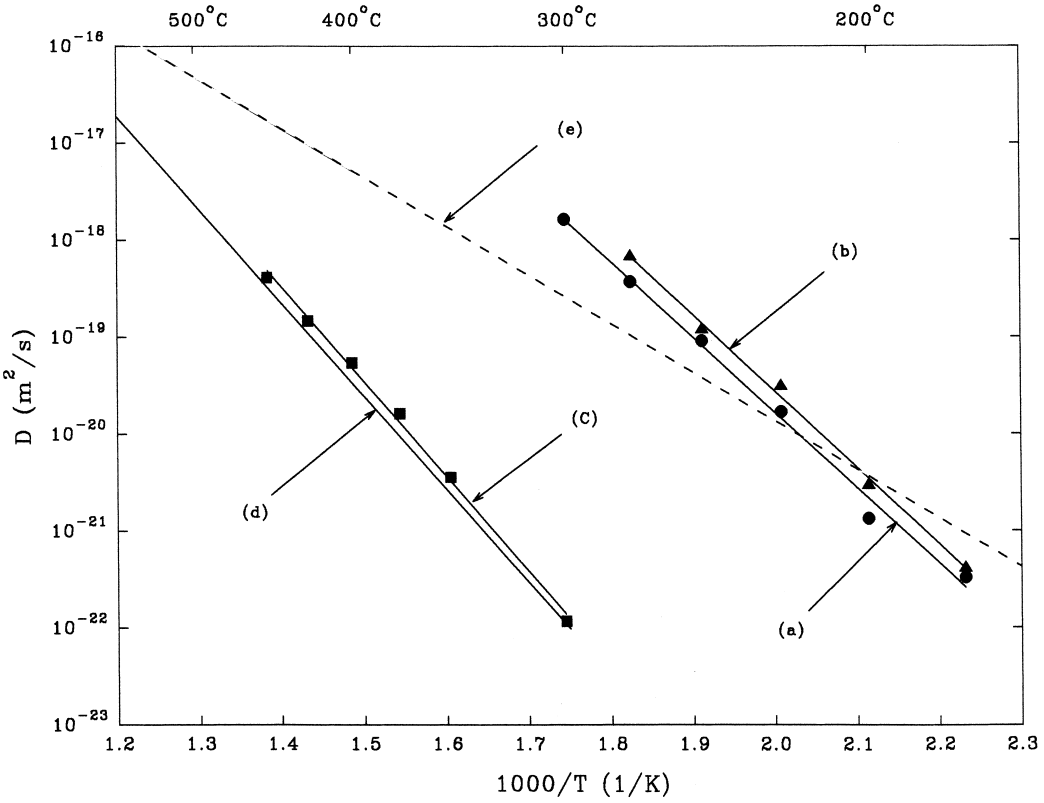

Fig. 6. The diffusion coefficients of oxygen in β-(Zr–20%Nb) alloy obtained from segregation experiments in this work (a) and obtained from oxide dissolution experiment on the same surface (b) [14]. Also shown are the diffusion coefficients of oxygen in α-(Zr–1%Nb) alloy obtained from oxide dissolution experiment (c) [14], the diffusion coefficients of oxygen in the bulk (d) and along the grain boundary (e) of α-(Zr) [15].

sion coefficients determined from the present study (curve (a), filled circles) and those obtained from our recent work by using oxide dissolution experiments (curve (b), filled triangles; [14]), indicates the good agreement achieved between these two measurements. The diffusion coefficients of oxygen in α-Zr, α-(Zr–1%Nb) alloy and along the grain boundary in α-Zr are also plotted in Fig. 6 for comparison. The diffusion coefficient data reported for diffusion along grain boundaries in α-Zr are from an extrapolation of data obtained at 400–700°C [15]. The α-(Zr–1%Nb) samples were prepared in a similar manner to the β-alloy in this work. It can be seen that the mobility of oxygen in the β-phase of the Zr–(20%Nb) alloy is higher than that in α-Zr and α-Zr–1%Nb alloy by more than three orders of magnitude at the operating temperature of a CANDU reactor (245–295°C). The O-diffusion coefficient along the grain boundaries in α-Zr, is still lower than that in the β-phase of Zr–20%Nb alloy by about one order of magnitude at reactor operating temperature. The results demonstrate that the migration of oxygen in β-phase actually dominates the movements of oxygen in the entire PT of a CANDU reactor during operation. Because of the complexity of possible effects in the α-(Zr–1%Nb) alloy relating to the chemical and physical state of the Nb in this alloy, we cannot attribute a detailed mechanism to the differences in diffusion coefficients in the α and β alloys. Likewise, spatially resolved measurements would be required to determine the contribution of grain boundary diffusion in the β-(Zr–20%Nb) alloy.

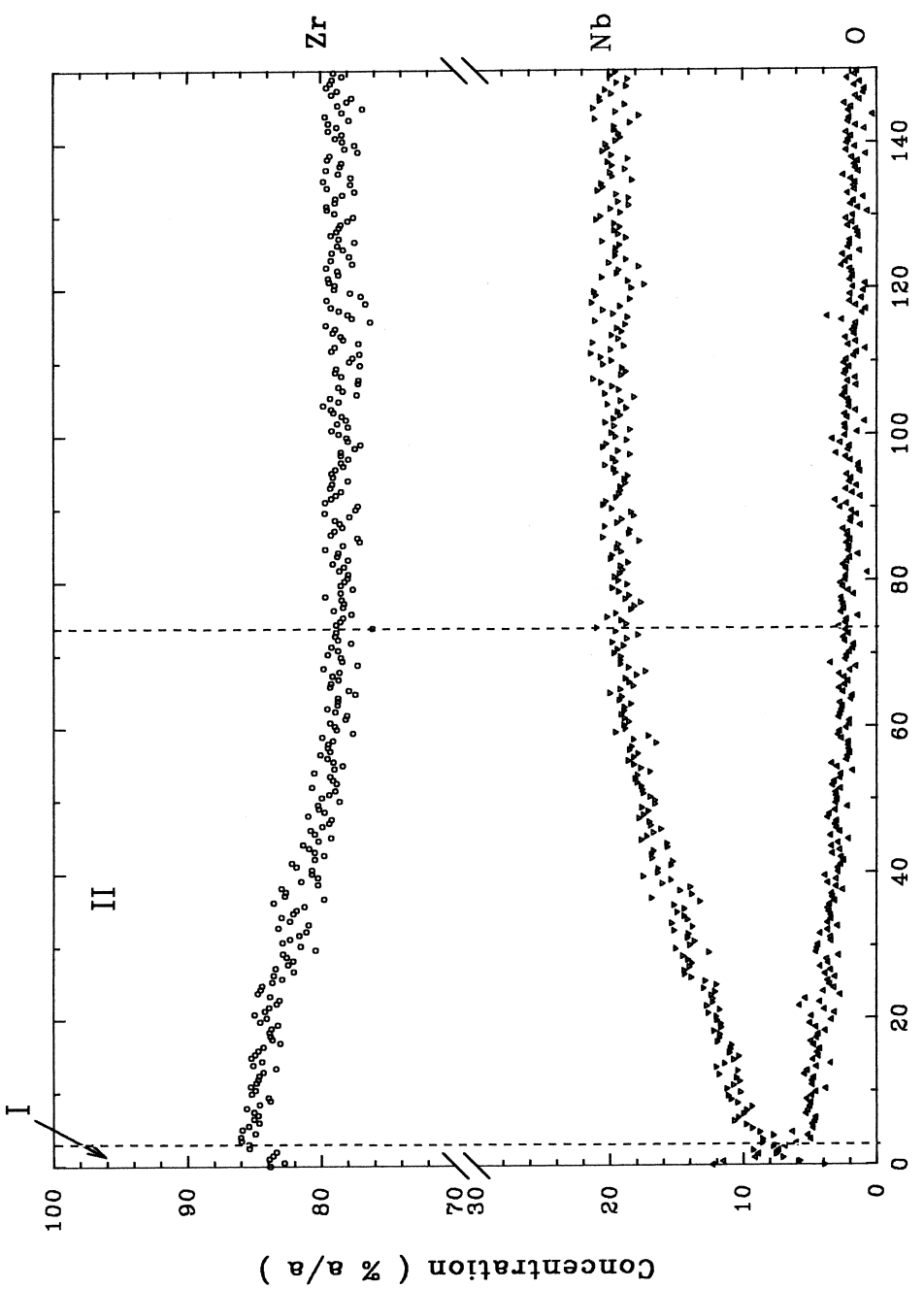

Fig. 7. Depth profile of concentrations of Zr, Nb and O after β-(Zr–20%Nb) alloy had been annealed at 450°C for 1200 s. Two distinguishable regions can been clearly seen near the surface.

3.3. Depth profiles after annealing

The depth profiles of O, Zr, and Nb were measured after annealing at various constant temperatures (250–650°C) and for different times (1 min to 24 h). Fig. 7 shows the depth profiles obtained after annealing at 450°C for 1200 s. It can be seen that there are two distinguishable regions formed beneath the surface. One is located within a few atomic layers of the surface and is associated with a sharp change of concentration of oxygen and niobium. We call it the segregation region or region I for convenience. A second region (II) occurs over greater depths into the bulk and is associated with a slow change in composition over more than a few hundred atomic layers.

Only segregation of oxygen occurs (region I) at annealing temperatures in the range 200–300°C. Very little change of Auger signals of Zr and Nb is observed in the surface region, and hence we conclude that oxygen migration is not accompanied by diffusion of zirconium and niobium. With annealing temperatures over 300°C, not only oxygen but also Nb and Zr atoms migrate. Fig. 8 shows depth profiles of the AES signals of Zr(MNV), Nb(MNV) and O (KLL) after isothermal experiments at 450°C for 0, 300 and 3000 s. (The zero time experiments indicates that the sample was heated rapidly at ~100°C/s and then immediately cooled (also at an ~100°C/s cooling rate) for subsequent sputter profiling.) The three horizontal dashed lines in Fig. 8 indicate, respectively, the intensities of the Zr(MNV),

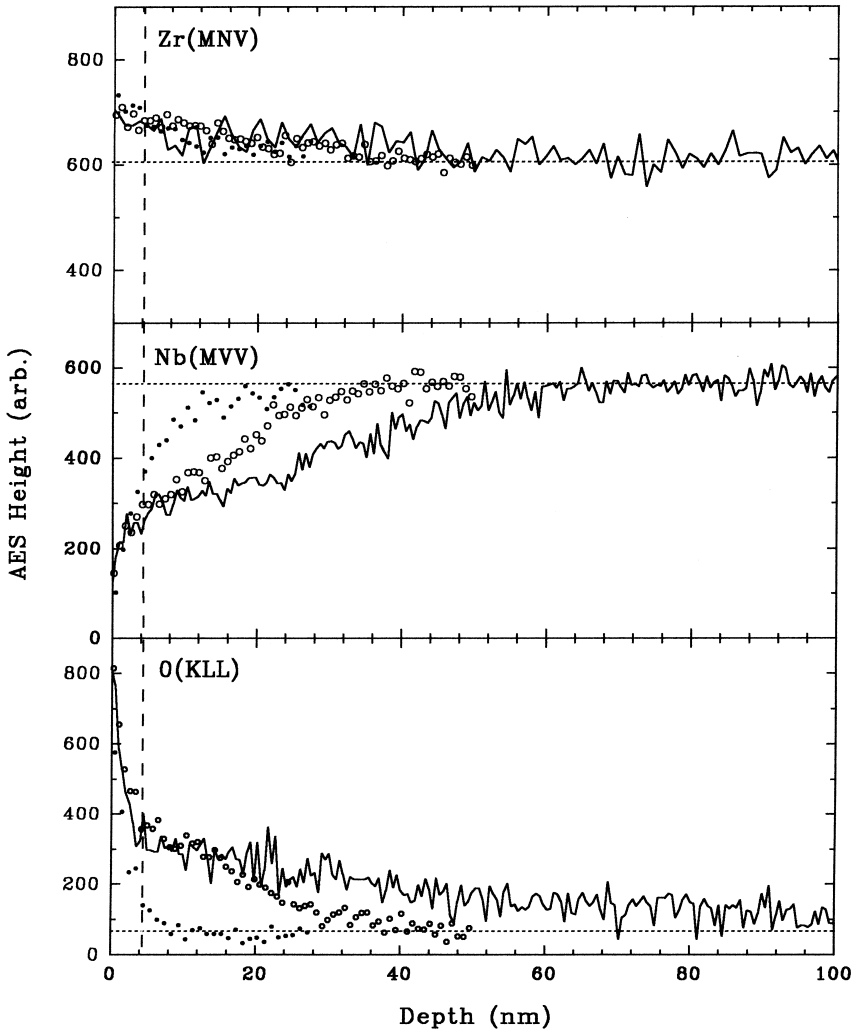

Fig. 8. Depth profiles of intensities of Zr(MNV), Nb(MVV) and O (KLL) Auger transitions on the surface of β-(Zr–20%Nb) alloy after annealing at 450°C for 0 (filled circles), 300 (open circles) and 3000 (solid lines) s. Three horizontal dashed lines indicated the intensities of Zr(MNV), Nb(MVV) and O (KLL) before the annealing experiments.

Nb(MNV) and O (KLL) Auger transitions before the annealing experiments; they are therefore characteristic of the bulk concentrations of the three elements. It is clear that significant changes of composition occur near the surface (within about 50 nm) as the samples are annealed. The segregation region (or region I), which is identified by a sharp change of composition (particularly of O and Nb) is always located within the first few atomic layers or a few nm near the surface, no matter how long the annealing time is. The *location* of this feature was also not changed by varying the annealing conditions. This was confirmed by depth profiles on samples after annealing at various temperature and for different times. It as interesting to note that the sharp change of composition in this region occurs very rapidly, even the 'zero time' anneal at 450°C producing most of the compositional changes observed at much longer times. The composition at the surface changes with the annealing temperature and time as has been illustrated in Fig. 2.

Turning now to the second, deeper region (II), there are several differences compared to the first region (I):

1. As shown in Fig. 7 the depth of the region over which the enrichment of Zr and O and depletion of Nb occur, is much greater than that of region I.
2. In contrast to region I, the width of region II, as shown in Table 3, increases with increasing annealing temperature and time.
3. The extent of the accumulation of O and Zr and depletion of Nb in this region depends upon the annealing temperature and time.

3.4. Discussion

As mentioned above, segregation of oxygen to the surface of the Zr–2.5Nb alloy occurs above 200°C. Generally speaking, there are two possible driving forces for surface segregation: the favourable energetics of the interaction of segregating atom with the free (dangling) bonds at the substrate surface, and the liberation of elastic energy at the surface, if the decrease of lattice stress associated with segregation is high. It is pertinent to note here that no oxygen segregation has been detected on the surfaces of α-Zr or α-Zr–1%Nb alloy. If we assume that the energetics of formation of chemical bonds between O and Zr atoms at the surface are similar in pure Zr and the alloy, then the segregation of O to the surface of the β-alloy cannot be attributed to this effect. It is however well known [15] that the solubility of oxygen in the β-Zr phase is much lower than in the α-Zr phase, although no room temperature data are currently available. It is therefore possible that the elastic energy of oxygen in the bulk of the metastable phase β-phase is high, which would be consistent with the low solubility, and this might be the dominant driving force for oxygen segregation.

As mentioned in the previous section, Zr atoms migrate to the surface region and Nb atoms move away from the surface when the temperature is over 300°C. It is well known that below the monotectoid temperature (610°C), the β-(Zr–20%Nb) phase is unstable and will transform to different mixtures of the following phases: α, ω, β_{cnr} and β_{Nb}, where the α and ω phases contain lower concentrations of Nb and the β_{cnr} and β_{Nb} phases contain higher concentrations of Nb [1]. Fig. 9 indicates the isothermal transition behaviour (TTT curve) of a bulk sample of Zr–19 wt% Nb alloy cooled from 850°C. We have heated the sample at various rates from 0.3 to 5°C/s. According to the TTT curve in Fig. 9, the $\beta \rightarrow \beta_{cnr} + \omega$ transition will occur in the sample at about 450°C at a heating rate of 0.3°C/s, but will not occur at 1 and 5°C/s heating rates at any experimental temperature. No significant differences in the changes of surface concentration were observed with various heating rates, except for a shift of a few degrees to higher temperature when the heating rate was increased from 0.3 to 5°C/s. This is the expected kinetic behaviour. Therefore, the bulk phase transition does not seem to affect the changes that occur in the various surface concentrations during heating.

Although the segregation process is completed in a relatively short time (region I), the changes in the composition in the second region (II) continue to develop as long as the annealing time is increased (Fig. 8). During annealing, region II which also contains higher Zr and O and lower Nb concentrations than characteristic of the bulk expands into the bulk. This process cannot be described as surface segregation, because of its large depth.

Table 3
The depth (nm) of region II at various isothermal annealing temperatures and times

Annealing time (s)	300°C	350°C	450°C	475°C	570°C
0			6		135
100			21.5	30–40	
300			30	55–60	
1200			52		320
3000			60		
3800	10	20			
38 000	21–25				

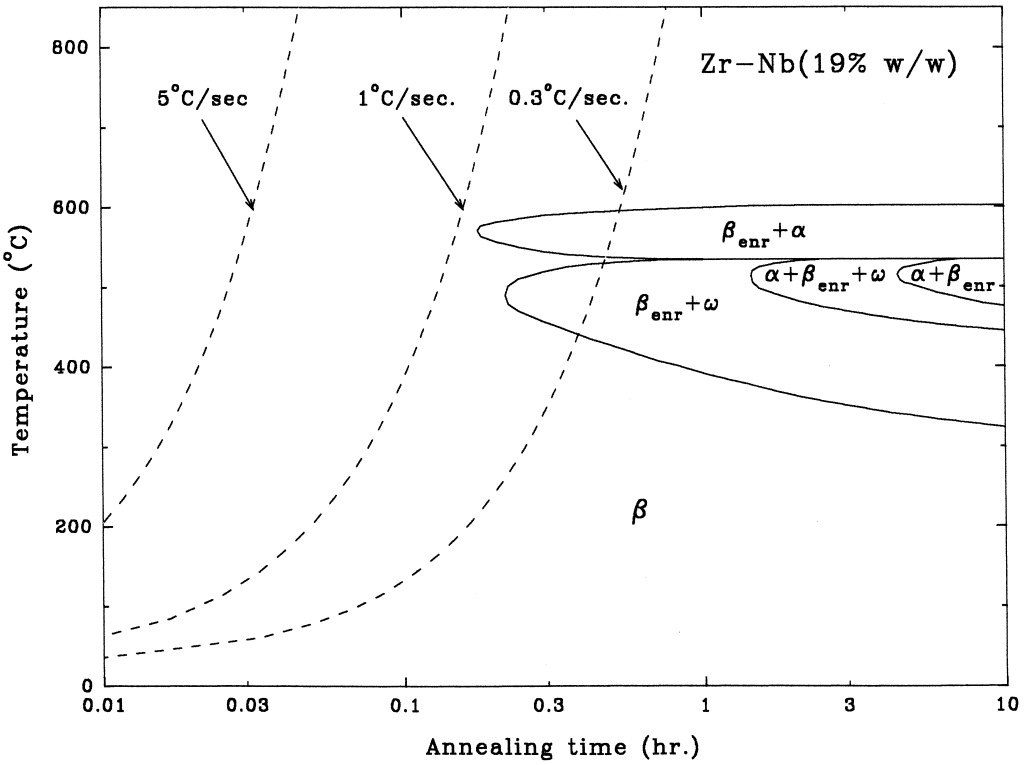

Fig. 9. The isothermal transformation behaviour of β-(Zr–19 wt% Nb) alloy cooled from 850°C. Three dashed lines indicate the three different heating rate (0.3, 1 and 5°C/s, respectively) used in our experiments.

Probably, this is related to the phase transitions mentioned above. The high value of the Zr/Nb ratio in the segregated layers (region I) might facilitate the initiation of the $\beta \rightarrow \alpha$ or ω phase transitions. With continual annealing, the low Nb concentration containing phase which is initiated near the surface, grows towards the bulk, creating the second region with a higher Zr concentration. Since the second region is essentially related to the growth of a low concentration Nb phase, the oxygen concentration in this region will increase with increasing Zr concentration, as has been demonstrated in the depth profile results (Fig. 8).

Finally we note the small 'recovery' in the Nb concentration at high temperatures. This might be attributable to the fact that above ~610°C (the monotectoid temperature), the β-(Zr–20%Nb) phase becomes more stable.

4. Summary

The segregation and enrichment of O and Zr and the simultaneous depletion of Nb has been observed to occur in two distinct regions of a β-(Zr–20%Nb) alloy upon annealing above 200°C. Segregation of Zr and O and depletion of Nb occur in the top few nm and more gradual changes that cannot be attributed to segregation, occur over the next few to a few hundred nm below the surface. The first region (region I, the segregation region), which is restricted to the first few atomic layers, is attributable to the segregation of oxygen and then Zr. The second region (region II), occurs beneath the segregation region and extends to a much greater depth than region I, and might result from alloy phase transitions initiated in region I. The segregation and enrichment of O and Zr and the depletion of Nb were mainly controlled by the annealing temperature and time. The diffusion coefficient of oxygen in the Zr–20%Nb β-phase obtained from the rate of segregation of oxygen, is in good agreement with those obtained from oxide dissolution measurements.

Acknowledgements

The authors gratefully acknowledge the financial support from Candu Owners Group (COG), the Natural Sciences and Engineering Research Council of Canada (NSERCC) and the Ontario Centre of Materials Research (OCMR).

References

[1] B.A. Cheadle, The physical metallurgy of zirconium alloys, CRNL-1208 Metallurgical Engineering Branch, Chalk River Nuclear Laboratories, Chalk River, Ontario, October, 1974.
[2] R.L. Tapping, T.S. Gendron, RC-101 Chalk River Nuclear Laboratory, COG-88-136, December, 1988.
[3] V.F. Urbanic, Chalk River Nuclear Laboratory, CRNL-2950, OH DND GEN 85431, October 1986.
[4] Y.P. Lin, private communication.
[5] R.S. Polizzotti, J.J. Burton, J. Vac. Sci. Technol. 14 (1977) 347.
[6] C.-S. Zhang, B. Li, P.R. Norton, J. Nucl. Mater. 223 (1995) 238.
[7] C.-S. Zhang, B. Li, P.R. Norton, J. Nucl. Mater. 199 (1993) 231.
[8] C.-S. Zhang, B. Li, P.R. Norton, J. Alloys Compounds 231 (1995) 354.
[9] C.-S. Zhang, B.J. Flinn, I.V. Michell, P.R. Norton, Surf. Sci. 264 (1991) 1.
[10] L.E. Davis, N.C. Macdonald, P.W. Palmberg, G.E. Riach, R.E. Weber, Handbook of Auger Electron Spectroscopy, Physical Electronics Division, Perkin–Elmer, Eden Prairie, 1975.
[11] I.V. Mitchell, G.R. Massoumi, W.N. Lennard, S.Y. Tong, P.F.A. Alkemade, K. Griffiths, S.J. Bushby, P.R. Norton, Nucl. Instrum. and Meth. B 45 (1990) 107.
[12] N.S. McIntyre, Private communication.
[13] A. Benninghoven, Secondary Ion Mass Spectrometry, Basic Concepts, Instrumental Aspects, Wiley, New York, 1987.
[14] C.-S. Zhang, P.R. Norton, to be published.
[15] I.G. Ritchie, A. Atrens, J. Nucl. Mater. 67 (1977) 254.